Frequency Synchronization in Frequency Domain OFDM-IM based WLAN Systems

Lalitha H, and Navin Kumar

***Abstract*—The next-generation of wireless local area network systems are being conceptualized with new applications, smart devices and use cases which mandate unprecedented levels of high data rates, spectral efficiency, reliability, low latency and high energy efficiency. The index modulated orthogonal frequency division multiplexing (OFDM-IM) stands out as the most endearing candidate for physical layer modulation technique which provides a smooth transit to green communications. However, OFDM-IM being a multicarrier technique similar to classical OFDM is also very sensitive to frequency synchronization errors and needs to be addressed on priority. In this article, a novel algorithm is proposed which estimates and corrects the carrier frequency offset at the receiver and the algorithm's performance is compared with two frequency domain variants of OFDM-IM and the classical OFDM under the same channel conditions and the simulation results show that our algorithm is not only capable of meeting the standard requirement of ±20ppm but can handle higher offsets till ±30ppm.**

***Index Terms*—carrier frequency offset, cyclic prefix, enhanced subcarrier index modulation, generalized index modulation, RF-Impairment.**

I. Introduction

OFDM is an implicit modulation technique utilised in most of the mobile and wireless communication standards and systems [1] such as third generation partnership project (3GPP) 5G new radio (NR) [2], IEEE 802.11 Wi-Fi standards starting from 802.11a Wi-Fi 2 to the latest WLAN standard Wi-Fi 6 [3], Long-term evolution (LTE) [4], Worldwide interoperability for microwave access (WiMAX) technology IEEE 802.16d/e [5], HIPERLAN/2 [6]. It has successfully flourished in all these systems owing to its merits of high data rate, effective resistance towards interference, simple single tap frequency domain equalization. However, the OFDM technique is limited by higher peak to average power ratio (PAPR), high sensitivity to timing and frequency synchronization errors [7].

The emerging next-generation of wireless networks (5G and beyond) are being designed with exceptional levels of very high data rates, reliability, low latency and there is also an urgent need to transit for greener communications with ubiquitous use cases [8]. The escalating teletraffic scenario has given rise to the challenging prospects in the research arena for advanced modulation schemes and waveforms which are more efficient in terms of both spectrum and energy with reliability [9]. Orthogonal frequency division multiplexing with index modulation (OFDM-IM) [10], similar to classical OFDM is a physical layer multi-carrier transmission technique with sparse symbol mapping, has garnered a lot of research interest in both industry and academia [11]. The index modulation (IM) extends the spatial modulation concept in the frequency domain, providing an additional index dimension with amplitude and phase constellation symbol to carry more data, which leads to additional diversity gain [12]. This flexible structure of IM enables us to create more energy friendly, transmission signals which is the utmost desirable attribute [13]. Thus, incorporating IM with OFDM results in OFDM-IM. The main idea in this technique is to utilize only a subset of the subcarriers and its indices to carry the data symbols while the rest are not used. This technique in general saves the transmitted power and the bit error rate (BER) performance is improved in comparison to classical OFDM [14]. Since only partial subcarriers are used to carry the data and the indices of these tones carrying additional data are extracted without any energy utilization, OFDM-IM technique enhances the system capability to attain the same throughput as classical OFDM by employing only partial resources. IM technique can be utilized in the time domain, frequency domain, spatial domain or the code domain on time slots, subcarriers, antennas and channel state variations respectively. The IM technique applied on the orthogonally spaced subcarriers are referred as frequency-domain IM (FD-IM).

The subcarriers in OFDM-IM are categorized into two types as data or active subcarriers and unused or inactive subcarriers, with active indices exploited to implicitly convey information bits [16]. However, OFDM-IM being a multi-carrier system similar to a classical OFDM, has inherited the sensitivity towards the carrier frequency offset, Any frequency error present distorts the orthogonality between the subcarriers resulting in inter carrier interference (ICI) which has double penalty effect of not only reducing the amplitude levels but also degrading the system performance [17].

It is a well-known fact that effective carrier frequency offset (CFO) estimation and compensation techniques are critical to a multi carrier system. Any algorithm to be designed needs to meet the standard prescribed limits set by IEEE 802.11standard which is typically ±20ppm in most WLAN standards [18]. The

Manuscript received April 18, 2023; revised May 24, 2023. Date of publication August 29, 2023. Date of current version August 29, 2023. The associate editor prof. Gordan Šišul has been coordinating the review of this manuscript and approved it for publication.

Lalitha H is with the Amrita School of Engineering, Amrita Vishwa Vidyapeetham, and Bangalore Institute of Technology. N. Kumar is with the Amrita School of Engineering, Amrita Vishwa Vidyapeetham (e-mails: lalithahmohan@gmail.com, navin_kum3@yahoo.com).

Digital Object Identifier (DOI): 10.24138/jcomss-2023-0052

CFO compensation techniques are broadly classified as data aided (utilizing the training/synchronization sequences or pilot sequences) and data unaided. In this paper we are proposing a blind method to effectively eliminate the CFO introduced and two popular schemes of FD-IM, enhanced subcarrier-index modulated OFDM (ESIM-OFDM) and an enhanced generalized SIM-OFDM (EGSIM-OFDM) referred as GIM is used to demonstrate that our algorithm works irrespective of any scheme in FD-IM.

The rest of the sections in the article are structured as mentioned. Related work and the motivation for the work carried out are emphasized in section II. The OFDM-IM system model is explained with illustration in section III, the proposed detection algorithm is described in section IV, the simulation and results are discussed in the V section, while the proposed work is concluded in section VI.

II. Related Works and Motivation

Frequency synchronization has been extensively studied in OFDM systems, resulting in a wide range of CFO detection and compensation methods utilizing both data aided and blind approaches [21]-[25]. Even though a plethora of research has been conducted and published in the areas of OFDM-index modulation which confirms the advantages of OFDM-IM in comparison to conventional OFDM, giving considerate amount of potential applications, advantages and working principle [26]-[37] but most of the prevailing IM techniques are only assessed under ideal conditions and further very few research has been done on the impact of carrier frequency offset on its performance.

The authors of [38], have come up with the CFO estimation technique for the OFDM-GIM variant using the pilot and the unused data tones. Initially, the CFO is estimated using the preassigned pilot tones, and later the unused data tones in GIM-OFDM are detected using energy detection and then utilizing both the pilot and unused data tones the CFO is re-estimated. The major drawback of this technique lies in the detection of the unused data tones which vary in number and position of each sub block and any detection of an activated data subcarrier as unused data carrier results in additional errors and the threshold used in the energy detection varies with the signal-to-noise ratio (SNR) and needs to be properly chosen and since this algorithm also depends on preassigned pilot subcarriers reduces the spectral efficiency. The authors of [39] have come up with a theoretical approach to predict the Bit Error Rate accuracy of OFDM-IM schemes like OFDM Interleaved subcarrier index modulation (OFDM-ISIM) and OFDM adjacent subcarrier index modulation (OFDM-ASIM) in comparison to classical OFDM under the influence of CFO and Rayleigh fading channels but they do not provide any correction mechanism for the CFO.

In [40], the authors have demonstrated bit error rate performance against the varying SNR for frequency domain IM schemes of GIM and subcarrier index modulation (SNM) with radio frequency (RF) impairments like carrier offset and IQ imbalance and have shown through computer simulations that even though the IM scheme provide higher spectral efficiency but they are sensitive to RF impairment like CFO and IQ imbalance like classical OFDM systems and no method are suggested to overcome these RF impairment. Authors in [41] Proposes a more precise analytical result related to the bit error rate (BER) performance analysis methodology for OFDM-IM based on Craig's formula instead of the exponential approximation where they have derived the average block error rate (BLER) and BER in closed form. But they do not consider any of the RF impairments into consideration when plotting average BLER and BER with respect to the ratio of transmit power to noise power (P_t/N_o). In [42], the authors have studied the achievable rate with an M-ary constellation of OFDM-IM impaired with Gaussian noise and with the complete information of channel impulse response known at the receiver , they have also come up with an interleaving technique applied to the subblock grouping in OFDM-IM which exploits the diversity gain better in a frequency selective fading channel and hence IM outperforms the conventional OFDM systems under small M (PSK schemes rather than QAM modulation techniques) and for certain intervals of SNR. In [43], the authors have come up with a multiple mode transmission scheme (MM-OFDM-IM)) wherein the sections of subcarriers can carry different modes and additional data bits are carried through permutation of the multiple modes. They have also proposed a detector based on subcarrier wise detection. But the major drawback of this scheme comes in the presence of CFO impairment as a strong ICI will be experienced similar to OFDM because all the subcarriers are filled with non-zero values, and no scheme to mitigate the ICI is proposed. In [44], the researchers have analyzed the capability of ESIM-OFDM using Schmidl and Cox algorithm synchronizer in the presence of Gaussian noise and Rayleigh fading channel and have come up with the threshold selection but it is not dependent on E_b/N_o and does not address the synchronization issues.

In [45], the authors have proposed a new variant of OFDM Index Modulation titled OFDM with all index modulation (OFDM-AIM) wherein the symbol bits used in OFDM-IM is eliminated by replacing the PSK/QAM modulator constellation by subblock modulator and they suggest that to accomplish the high diversity gain, the subblocks with higher order set design must be utilised and they propose an algorithm to construct the subblocks set with maximum order diversity. In [46], hybrid OFDM-IM is proposed by the authors, wherein the mode can be switched alternately either to classical OFDM or OFDM-IM based on the channel conditions. If the SNR values range from low to medium range, then normal OFDM is used for transmission and when the SNR is high OFDM-IM is used. In both cases for simulations, Rayleigh and Rician fading channels is considered while plotting BER vs. SNR, no other RF-Impairment is considered. Against the above background, in the current article, we have recommended a novel compensation

Algorithm which estimates and corrects the frequency error. In this work, the error performance of two prominent frequency domain IM schemes: enhanced subcarrier index modulation (ESIM) and generalized index modulation (GIM) are evaluated along with the classical OFDM for three different CFO limits set at ±20ppm, ±25ppm and ±30ppm under the influence of Rayleigh scattering and AWGN channel conditions. The simulation results show that the proposed method is independent of the modulation schemes used and performs very well for not only the prescribed standard limit of ±20ppm but

even for higher offsets of ±25ppm and demands better signal quality when the CFO limit is further raised to ±30ppm.

Notation: In this article the symbols $()^{T}$, $()^{‡}$ and $()^{*}$ represent the transpose, conjugate transpose and complex conjugate respectively.

III. OFDM-IM System Model

The block schematic of a frequency domain OFDM-IM system is illustrated in Fig. 1. The FD–IM is capable of carrying the extra data bits, particularly on the locations or indices of the activated data tones, without the need of additional energy for transmission. The '*s*' data bits to be carried by the symbol is fed to a bit splitter which equally splits the $\boldsymbol{s}$ bits into *G* groups where each group are allotted a set of $\boldsymbol{p}$ bits which are further segregated into two subgroups of *p1* index bits and *p2* symbol bits. The index bits determine the positions of the data tones which carry the data symbols which are generated using the data bits from symbol mapping, and later all these subgroups are concatenated and fed to an OFDM symbol formation block which allocates all the subcarriers frequencies in the OFDM symbol and passed to the N-IFFT block resulting in a time domain OFDM signal of *N* samples to which a sufficient length guard interval is pre-appended based on the maximum channel delay spread time

In enhanced subcarrier index modulation OFDM (ESIM-OFDM), the subcarriers are clustered using two successive data tones and in every group only one data tone is activated and the other one is kept as an unused subcarrier and the indices of these used data carriers carries the additional data. In the GIM frequency domain IM technique, the data tones grouped into OFDM subgroups are not restricted to two. In every OFDM subgroup of size $\boldsymbol{p}$, it is further split into index bits represented as *p1* and symbol bits as *p2*. Index bits specify the locations of the activated data tones which carry the mapped symbol bits *m1* and *m2* explicitly and the other data tones are retained as unused data subcarrier *u1* and *u2* as shown in the look up Table I where *p1* is chosen to be two and subgroup size is four.

TABLE I
LOOKUP TABLE FOR GIM-OFDM

INDEX BITS	DATA LOCATION	SUBGROUPS
[0,0]	[1,2]	[m1,m2,u1,u2]
[0,1]	[2,3]	[u1,m1,m2,u2]
[1,1]	[1,4]	[m1,u1,u2,m2]
[1,0]	[3,4]	[u1,u2,m1,m2]

Let $\boldsymbol{x'}_i$ be the input data vector of length *N*, and $\boldsymbol{x'}_{i,L}$ be the guard interval of length *L* which is pre-appended to the input vector block, making the transmitted signal cyclic in nature.

$$\boldsymbol{x'}_i = [x_i(0), x_i(1), x_i(2), \ldots\ldots\ldots\ldots x_i(N-1)]^{T} \quad (1)$$

$$\boldsymbol{x'}_{i,L} = [x_i(N-L), \ldots.\ldots x_i(N-2), x_i(N-1)]^{T} \quad (2)$$

Then the i[th] signal vector transmitted can be mathematically represented as:

$$\boldsymbol{x}_i = \begin{bmatrix} \boldsymbol{x'}_{i,L} \\ \boldsymbol{x'}_i \end{bmatrix} \quad (3)$$

The i[th] signal block captured at the receiver end can be represented as:

$$\boldsymbol{y}_i = \boldsymbol{H}\begin{bmatrix} \boldsymbol{x}_{i-1,L} \\ \boldsymbol{x}_i \end{bmatrix} e^{j2\pi\frac{i(N+L)\varphi}{N}} \boldsymbol{D}(\varphi) + \boldsymbol{w}_i \quad (4)$$

where $\boldsymbol{H}$ is a Toeplitz matrix with (N+L) x (N+2L) size and the first row is $[h(L), \ldots\ldots\ldots, h(0), 0 \ldots 0]$, the first column is $[h(L), 0, \ldots\ldots.0]^{T}$ and the channel coefficients are represented as h(0), h(1), h(2),…….h(L). The normalized carrier frequency offset φ is defined as the product of NΔf/Fs , where Δf is the offset in Hz and F_s is the sampling frequency.

The diagonal matrix $\mathbf{D}(\varphi)$ and AWGN vector $\boldsymbol{w}_i$ of the i[th] noise block with variance of σ_i^2 are given as in equation (5) and (6)

$$\boldsymbol{D}(\varphi) = diag\{\, 1, e^{\frac{j2\pi\varphi}{N}}, \ldots\ldots\ldots, e^{\frac{j2\pi(N+L-1)\varphi}{N}} \,\} \quad (5)$$

$$\boldsymbol{w}_i = [w_i(0), w_i(1), \ldots\ldots\ \ w_i(N+L-1)]^{T} \quad (6)$$

IV. Proposed CFO Estimation Algorithm

A remodulated vector $\widetilde{\boldsymbol{y}}_i$ may be created by concatenating the last *N* samples of the previous received symbol $\boldsymbol{y}_{i-1}$ with the initial *L* entries of the current received symbol $\boldsymbol{y}_i$. The remodulated signal vector constructed so is also of same length as a conventional OFDM symbol length of N+L. Thus two received symbols are required to create a single remodulated vector. Its cyclic structure is retained and can be utilized even in a multipath environment [47].

The remodulated vector can be represented mathematically as in equation (7):

$$\widetilde{\boldsymbol{y}}_i \triangleq [y_{i-1}(L), \ldots y_{i-1}(N+L-1), y_i(0), \ldots y_i(L-1)]^{T} \quad (7)$$

The remodulated signal constructed at the receiver impaired with channel, carrier offset and noise can be represented as

$$\widetilde{\boldsymbol{y}}_i = \boldsymbol{H}\begin{bmatrix} \boldsymbol{x}_{i-1} \\ \boldsymbol{x}_{i,L} \end{bmatrix} e^{j2\pi\varphi\frac{i(N+L)-N}{N}} \boldsymbol{D}(\varphi) + \widetilde{\boldsymbol{w}}_i \quad (8)$$

where,

$\widetilde{\boldsymbol{w}}_i = [w_{i-1}(L), \ldots w_{i-1}(N+L-1), w_i(0), \ldots w_i(L-1)]^{T}$

Computing the autocorrelation matrix $\mathbf{R}_{rr}(\varepsilon)$ of the difference vector $\boldsymbol{r}_i(\varepsilon)$ where the variable ε is utilised in the offset calculation.

$$\mathbf{R}_{rr}(\varepsilon) = \mathrm{E}\{\, \boldsymbol{r}_i(\varepsilon)\ \boldsymbol{r}_i(\varepsilon)^{‡} \,\} \quad (9)$$

And, the difference vector $\boldsymbol{r}_i(\varepsilon) = \boldsymbol{y}_i - e^{j2\pi\varepsilon}\widetilde{\boldsymbol{y}}_i$ substituting the equations (4) and (8) in $\boldsymbol{r}_i(\varepsilon)$ can be represented as:

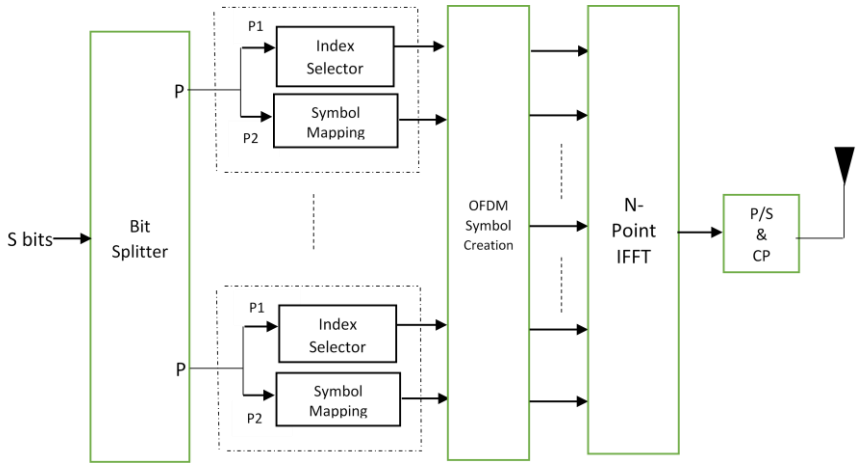

Fig. 1. Illustration of OFDM - IM System

$$\boldsymbol{r}_i(\varepsilon) = e^{j2\pi i\frac{(N+L)\varphi}{N}}\boldsymbol{D}(\varphi)\boldsymbol{H}\left(\begin{bmatrix}\boldsymbol{x}_{i-1,L}\\ \boldsymbol{x}_i\end{bmatrix} - e^{j2\pi(\varepsilon-\varphi)}\begin{bmatrix}\boldsymbol{x}_{i-1}\\ \boldsymbol{x}_{i,L}\end{bmatrix}\right) + \underbrace{(\boldsymbol{w}_i - e^{j2\pi\varepsilon}\widetilde{\boldsymbol{w}}_i)}_{\mathrm{n}_e} \tag{10}$$

Using equation (10), the auto correlation matrix $\mathbf{R}_{rr}(\varepsilon)$ is computed presuming both the signal vector and the noise vector are uncorrelated:

$$\boldsymbol{R}_{rr}(\varepsilon) = \sigma_x^2\boldsymbol{D}(\varphi)\boldsymbol{H}\boldsymbol{\varpi}\boldsymbol{H}^{\ddagger}\boldsymbol{D}(-\varphi) + \sigma_{\mathrm{n}_e}^2\boldsymbol{R}_{\mathrm{n}_e}(\varepsilon) \tag{11}$$

where $\boldsymbol{\varpi}$ is a matrix of size (N+2L) x (N+2L) represented by (11a) and with $\tau_1 = \cos(2\pi(\varepsilon-\varphi))$, $\tau_2 = 1 - e^{j2\pi(\varepsilon-\varphi)}$ and $\boldsymbol{R}_{\mathrm{n}_e}(\varepsilon)$ is a matrix of order (N+L) x (N+L) given in (11b), and the average signal power of the vector transmitted is σ_x^2

$$\boldsymbol{\varpi} = \begin{bmatrix} 2(1-\tau_1)I_L & 0 & 0 & \tau_2^* I_L & 0\\ 0 & 2I_L & 0 & 0 & \tau_2^* I_L\\ 0 & 0 & 2I_{N-2L} & 0 & 0\\ \tau_2 I_L & 0 & 0 & 2I_L & 0\\ 0 & \tau_2 I_L & 0 & 0 & 2(1-\tau_1)I_L \end{bmatrix} \tag{11a}$$

$$\boldsymbol{R}_{\mathrm{n}_e}(\varepsilon) = \begin{bmatrix} 2I_L & 0 & -e^{-j2\pi\varepsilon}I_L\\ 0 & 2I_{N-L} & 0\\ -e^{-j2\pi\varepsilon}I_L & 0 & 2I_L \end{bmatrix} \tag{11b}$$

The diagonal entries of $\boldsymbol{R}_{rr}(\varepsilon)$ are computed using the equation (11) and can be represented as

$$[\boldsymbol{R}_{rr}(\varepsilon)]_{k,k} = \begin{cases} 2(\zeta - \alpha_1\zeta_k) & if\ i \in C\\ 2\zeta + (2\sigma_{\mathrm{n}_e})^2 & otherwise \end{cases} \tag{11c}$$

where C is the set of indices of first L (0, 1. . . L-1) and the last L samples (N, N+1 . . . N+L-1) of the difference vector $\boldsymbol{r}_i$

$$\zeta \triangleq (\sigma_x)^2\sum_{l=0}^{L}|h(l)|^2 \tag{12}$$

$$\zeta_k = \begin{cases} (\sigma_x)^2\sum_{l=k+1}^{L}|h(l)|^2 & if\ 0 \le k \le L-1\\ (\sigma_x)^2\sum_{l=0}^{i-N}|h(l)|^2 & if\ N \le k \le N+L-1 \end{cases} \tag{13}$$

It is clear from equation (12) and (13) that both ζ and ζ_k are independent of parameters $\boldsymbol{\varepsilon}$ and φ and the cost function can be written as

$$\tilde{J}(\varepsilon) = \sum_{k\in C}[\boldsymbol{R}_{rr}(\varepsilon)]_{k,k} \tag{14}$$

Hence, the cost function is minimum when ε is equal to φ. And the closed form solution to efficient estimation of the CFO can be approximated in terms of autocorrelation matrix $\boldsymbol{R}_{rr}(\varepsilon)$ as equation (15) and S is the number of OFDM-IM symbols considered. Here, only S-1 symbols are considered as a minimum of 2 OFDM-IM is required to construct one remodulation vector.

$$\boldsymbol{R}_{rr}(\varepsilon) \approx \frac{1}{S-1}\sum_{i=1}^{S-1}\boldsymbol{r}_i(\varepsilon)\left(\boldsymbol{r}_i(\varepsilon)\right)^{\ddagger} \tag{15}$$

$$\boldsymbol{R}_{rr}(\varepsilon) \approx \frac{1}{S-1}\sum_{i=1}^{S-1}\sum_{k\in C}\left(\boldsymbol{r}_i(k) - e^{j2\pi\varepsilon}\tilde{\boldsymbol{r}}_i(k)\right)\left(\left(\boldsymbol{r}_i(k) - e^{j2\pi\varepsilon}\tilde{\boldsymbol{r}}_i(k)\right)^*\right) \tag{16}$$

The range for ε is set between (-0.5, 0.5) and the cost function can be re-written as

$$\hat{\varphi} = \arg \min_{\varepsilon \in (-0.5, 0.5)} \tilde{J}(\varepsilon) \tag{17}$$

The cost function $\tilde{J}(\varepsilon)$ is minimized by taking its derivative and equating it to zero. It is observed that for the set range, equation (16) has a unique minimum and coarse estimation or Level 1 (L1) estimate of the CFO estimation is given by

$$\hat{\varphi}_{L1} = \frac{1}{2\pi} angle \left[\sum_{i=1}^{S-1} \sum_{k \in c} \boldsymbol{y}_i(k) \left(\tilde{\boldsymbol{y}}_i(k) \right)^* \right] \tag{18}$$

Once the *L1* estimate is obtained, evaluate the equation (11c) and select only those indices within the *2L* length of the set *C* of the diagonal entries with minimum value such that the new length of $C_{min} < 2L$. Since the smaller diagonal entries have larger second order derivative. After choosing the C_{min}, compute the Fine estimate or Level 2 (L2) estimate using the equation (19):

$$\hat{\varphi}_{L2} = \frac{1}{2\pi} angle \left[\sum_{i=1}^{S-1} \sum_{k \in Cmin} \boldsymbol{y}_i(k) \left(\tilde{\boldsymbol{y}}_i(k) \right)^* \right] \tag{19}$$

The mean square error (MSE) is finally computed by taking the mean square difference between the computed offset and the introduced offset. *R* dictates the number of runs for which the algorithm is computed.

$$\text{MSE}(\varphi) = \frac{1}{R} \sum_{i=1}^{R} |\hat{\varphi}(i) - \varphi|^2 \tag{20}$$

V. Simulation Results and Discussion

The performance of the proposed algorithm was evaluated through computer simulations using MATLAB software, the evaluation was carried out for two variants of frequency-domain IM (FD-IM), namely the ESIM-OFDM and GIM-OFDM along with the classical OFDM. The simulation parameters chosen are tabulated in TABLE II.

TABLE II
Simulation Parameters

PARAMETERS	GIM/ESIM
FFT size (N)	64
Guard Interval (CP Length)	16
No. of subgroups in every symbol	16
Modulation type	BPSK
CFO	±20ppm, ±25ppm, ±30ppm
Channel	AWGN with Multipath Rayleigh fading
channel delay samples locations	[0,1,2,6,8]
channel tap power profile	[0.34,0.28,0.23,0.11,0.04]
No. of OFDM symbols (S)	10,50
No. of Runs	1000

The plots in Fig. 2 – Fig. 7 give the performance of the proposed algorithm as a function of mean square error with respect to varying SNR (dB) for classical OFDM, enhanced subcarrier index modulation and generalized index modulation.

Fig. 2 is the performance plot of MSE vs. SNR (dB) considering the total number OFDM symbols (block size) of 10 and introduced frequency error is ±20ppm. It is evident from the plot that there is a marginal improvement in the case of GIM and ESIM when compared to classical OFDM. Both in coarse estimation and fine estimation. Although coarse estimation suffers from error flooring after an initial decrease in MSE with an increase in SNR, it remains constant after 10dB and shows no improvement thereafter and remains fixed at close to 10^{-4}.

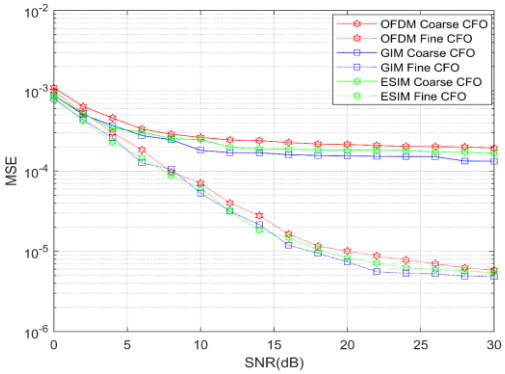

Fig. 2. MSE vs. SNR(dB) comparison for block size=10 ,CFO = ±20ppm

The error flooring characteristics are not seen in the fine estimate and MSE decreases further down with an increase in SNR and lies between 10^{-5} and 10^{-6}. Performance plot in Fig. 3 is similar to Fig. 2 but the frequency error parameter is increased to ±25ppm. It also displays a marginal improvement of index modulation in comparison to classical OFDM and the error flooring pattern can be observed in coarse estimation and the MSE lies between 10^{-5} and 10^{-6} consolidating that the proposed algorithm can handle higher frequency offsets with equal efficiency.

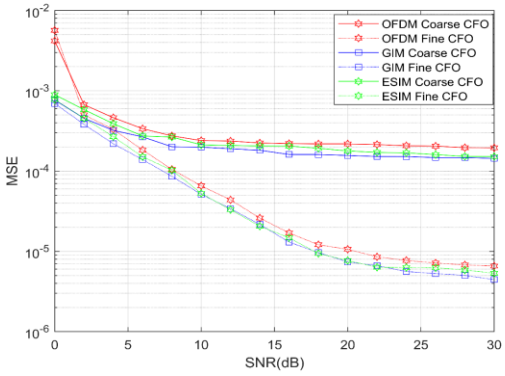

Fig. 3. MSE vs. SNR(dB) comparison for block size = 10, CFO = ±25ppm

In Fig. 4, we observe that as the block size is increased to 50 and the CFO is set to ±20ppm, the marginal difference between the 3 schemes vanishes and they all overlay on each other in both coarse and fine estimation. Although, fine estimation always outperforms coarse estimation and MSE decreases to greater than 10^{-6}. As the CFO is further increased to ±25ppm, the overlay pattern continues and MSE is close to 10^{-6} and not much difference to Fig. 4 is observed in Fig. 5.

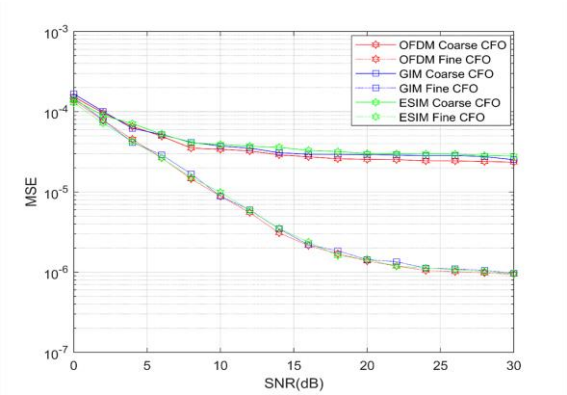

Fig. 4. MSE vs. SNR(dB) comparison for block size = 50, CFO = ±20ppm

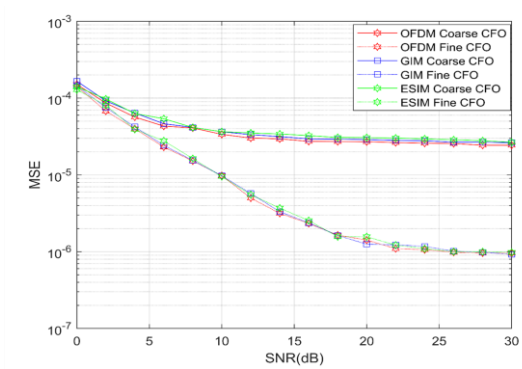

Fig. 5. MSE vs. SNR(dB) comparison for block size = 50, CFO = ±25ppm

Fig. 6 is the performance plot for block size 10 and the frequency error increased further to ±30ppm. And we observe that the classical OFDM suffers the most both in coarse and fine estimation and among the GIM and ESIM, ESIM outperforms, achieving an MSE greater than 10^{-2} for coarse estimation. For the case of fine estimation, the MSE decreases when the SNR is greater than 10dB for index modulation, OFDM scheme demands much better SNR greater than 15dB and overall they overlap, eventually demanding better signal quality as the frequency error is increased. At a high frequency error of ±30ppm, with an increase in block size to 50, the MSE of coarse lies between 10^{-4} and 10^{-5} while that of fine estimation achieves 10^{-6} as seen in Fig. 7.

Figs. 8 and 9 are the comparative graphs of our proposed algorithm with algorithms using pilot subcarriers and unused subcarriers to estimate the carrier frequency offset in ESIM and GIM variants. Our proposed algorithm clearly outperforms in estimating the CFO error irrespective of the CFO introduced. Whereas the algorithms based on pilot subcarrier showed slightly better performance at low SNR regions up to ±25ppm as compared to our proposed algorithm, But as the CFO limits are further pushed to ±30ppm, our proposed algorithm clearly out performs the other CFO estimations as observed in Fig. 9.

VI. CONCLUSION

OFDM-IM is capable of addressing the critical needs for a smooth transit to greener communications for Wi-Fi 6 and beyond technologies. However, it is also sensitive to frequency errors which needs to be addressed efficiently to utilize its full potential. Our proposed novel algorithm efficiently handles the frequency error by accurately estimating the CFO using the remodulated guard interval. The algorithm is independent of the modulation scheme employed or the variants of OFDM-IM used. The performance of the algorithm not only satisfies the prescribed standard limits but also work equally efficiently at higher offsets like ±25ppm. When the offset is further increased to ±30ppm, the proposed algorithm will perform but requires better SNR. Thus, the algorithm proposed work's for both OFDM-IM and Conventional OFDM, and WLAN systems can make use of OFDM-IM schemes to harness its complete potential.

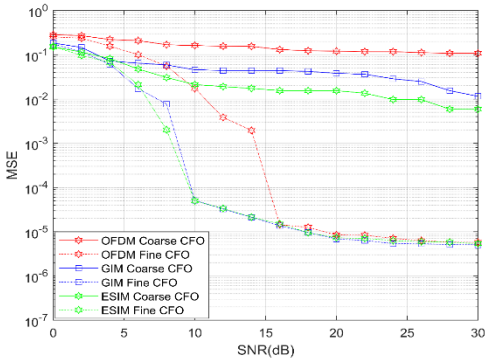

Fig. 6. MSE vs. SNR(dB) comparison for block size = 10, CFO = ±30ppm

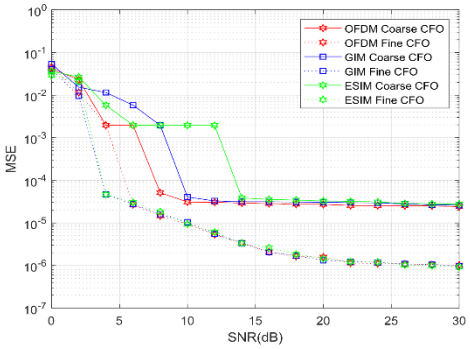

Fig. 7. MSE vs. SNR(dB) comparison for block size = 50, CFO = ±30ppm

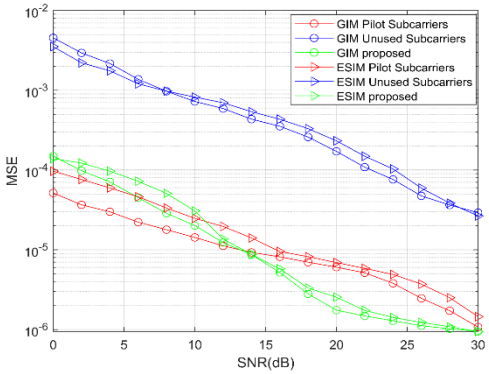

Fig. 8. MSE vs. SNR(dB) comparison result with different Algorithms , CFO = ±25ppm

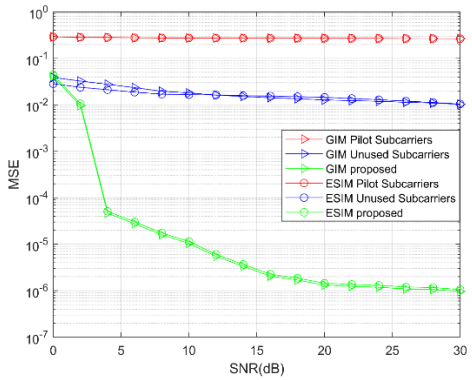

Fig. 9. MSE vs. SNR(dB) comparison result with different Algorithms , CFO = ±30ppm

REFERENCES

[1] J.S Bridle, Yong Soo Cho; Jaekwon Kim; Won Young Yang; Chung G. Kang, "Introduction to OFDM," in MIMO-OFDM Wireless Communications with MATLAB® , IEEE, 2010, pp.111-151, doi: 10.1002/9780470825631.ch4

[2] Mihai Enescu; Karri Ranta-aho, "Introduction and Background," in 5G New Radio: A Beam-based Air Interface , Wiley, 2020, pp.1-23, doi: 10.1002/9781119582335.ch1

[3] "IEEE Standard for Information Technology--Telecommunications and Information Exchange between Systems Local and Metropolitan Area Networks--Specific Requirements Part 11: Wireless LAN Medium Access Control (MAC) and Physical Layer (PHY) Specifications Amendment 1: Enhancements for High-Efficiency WLAN," in IEEE Std 802.11ax-2021 (Amendment to IEEE Std 802.11-2020) , vol., no., pp.1-767, 19 May 2021, doi: 10.1109/IEEESTD.2021.9442429.

[4] Ayman Elnashar; Mohamed A. El-saidny, "LTE and LTE-A Overview," in Practical Guide to LTE-A, VoLTE and IoT: Paving the way towards 5G , Wiley, 2018, pp.1-86, doi: 10.1002/9781119063407.ch1

[5] Marcos Katz; Frank H. P. Fitzek, "Introduction to WiMAX Technology," in WiMAX Evolution: Emerging Technologies and Applications, Wiley, 2009, pp.1-13, doi: 10.1002/9780470740118.ch1.

[6] Jamshid Khun-Jush, P. Schramm, U. Wachsmann and F. Wenger, "Structure and performance of the HIPERLAN/2 physical layer," Gateway to 21st Century Communications Village. VTC 1999-Fall. IEEE VTS 50th Vehicular Technology Conference (Cat. No.99CH36324), Amsterdam, Netherlands, 1999, pp. 2667-2671 vol.5, doi: 10.1109/VETECF.1999.800270.

[7] T. Kebede, Y. Wondie, J. Steinbrunn, H. B. Kassa and K. T. Kornegay, "Multi-Carrier Waveforms and Multiple Access Strategies in Wireless Networks: Performance, Applications, and Challenges," in IEEE Access, vol. 10, pp. 21120-21140, 2022, doi: 10.1109/ACCESS.2022.3151360.

[8] Anwer Al-Dulaimi; Xianbin Wang; Chih-Lin I, "Waveform Design for 5G and Beyond," in 5G Networks: Fundamental Requirements, Enabling Technologies, and Operations Management, IEEE, 2018, pp.51-76, doi: 10.1002/9781119333142.ch2.

[9] E. Basar, M. Wen, R. Mesleh, M. Di Renzo, Y. Xiao and H. Haas, "Index Modulation Techniques for Next-Generation Wireless Networks," in *IEEE Access*, vol. 5, pp. 16693-16746, 2017, doi: 10.1109/ACCESS.2017.2737528.

[10] C. Xu et al., "Space-, Time-and Frequency-Domain Index Modulation for Next-Generation Wireless: A Unified Single-/Multi-Carrier and Single-/Multi-RF MIMO Framework," in IEEE Transactions on Wireless Communications, doi: 10.1109/TWC.2021.3054068.

[11] E. Başar, Ü. Aygölü, E. Panayırcı and H. V. Poor, "Orthogonal Frequency Division Multiplexing With Index Modulation," in IEEE Transactions on Signal Processing, vol. 61, no. 22, pp. 5536-5549, Nov.15, 2013, doi: 10.1109/TSP.2013.2279771

[12] S. Sugiura, T. Ishihara and M. Nakao, "State-of-the-Art Design of Index Modulation in the Space, Time, and Frequency Domains: Benefits and Fundamental Limitations," in IEEE Access, vol. 5, pp. 21774-21790, 2017, doi: 10.1109/ACCESS.2017.2763978.

[13] M. Irfan and S. Aïssa, "On the Spectral Efficiency of Orthogonal Frequency-Division Multiplexing with Index Modulation," 2018 IEEE Global Communications Conference (GLOBECOM), Abu Dhabi, United Arab Emirates, 2018, pp. 1-6, doi: 10.1109/GLOCOM.2018.8647972.

[14] X. Cheng, M. Zhang, M. Wen and L. Yang, "Index Modulation for 5G: Striving to Do More with Less," in IEEE Wireless Communications, vol. 25, no. 2, pp. 126-132, April 2018, doi: 10.1109/MWC.2018.1600355.

[15] K. Kim, "PAPR Reduction in OFDM-IM Using Multilevel Dither Signals," in IEEE Communications Letters, vol. 23, no. 2, pp. 258-261, Feb. 2019, doi: 10.1109/LCOMM.2019.2892103.

[16] Q. Ma, Y. Xiao, L. Dan, P. Yang, L. Peng and S. Li, "Subcarrier Allocation for OFDM With Index Modulation," in IEEE Communications Letters, vol. 20, no. 7, pp. 1469-1472, July 2016, doi: 10.1109/LCOMM.2016.2560171.

[17] R. Sharma, H. Lalitha and N. Kumar, "Design and development of non data aided estimation algorithm for carrier frequency-offset and I/Q imbalancing in OFDM-based systems," 2013 Tenth International Conference on Wireless and Optical Communications Networks (WOCN), 2013, pp. 1-4, doi: 10.1109/WOCN.2013.6616177.

[18] National Instruments, "Introduction to 802.11ax High-Efficiency Wireless" [Online]. http://www.ni.com/white-paper/53150/en/.

[19] Haesik Kim, "Orthogonal Frequency-Division Multiplexing," in Wireless Communications Systems Design , Wiley, 2015, pp.209-238, doi: 10.1002/9781118759479.ch7.

[20] Weile Zhang and Qinye Yin," Blind Carrier Frequency Offset Estimation for MIMO-OFDM With Constant Modulus Constellations via Rank Reduction Criterion", IEEE TRANSACTIONS ON VEHICULAR TECHNOLOGY, VOL. 65, NO. 8, AUGUST 2016

[21] Chang-Yi Yang, Yu-Li Chen, and Hai-Yan Song" Adaptive Carrier Frequency Offset and Channel Estimation for MIMO-OFDM Systems", in Proc. Of 30th International Conference on Advanced Information Networking and Applications Workshops, 2016, pp. 949-954.

[22] Chang-Yi Yang, Yu-Li Chen, and Hai-Yan Song" Adaptive Carrier Frequency Offset and Channel Estimation for MIMO-OFDM Systems", in Proc. Of 30th International Conference on Advanced Information Networking and Applications Workshops, 2016, pp. 949-954.

[23] F. Gao, Y. Zeng, A. Nallanathan, and T.-S. Ng, "Robust Subspace Blind Channel Estimation for Cyclic Prefixed MIMO OFDM Systems: Algorithm, Identifiability and Performance Analysis," IEEE Journal on Selected Areas in Commun., vol. 26, no. 2, pp. 378-388, Feb. 2008.

[24] L. H and N. Kumar, "Blind Frequency Synchronization for WLAN MIMO OFDM Systems," 2020 2nd PhD Colloquium on Ethically Driven Innovation and Technology for Society (PhD EDITS), 2020, pp. 1-2, doi: 10.1109/PhDEDITS51180.2020.9315307.

[25] R. Fan, Y. J. Yu and Y. L. Guan, "Generalization of Orthogonal Frequency Division Multiplexing With Index Modulation," in IEEE Transactions on Wireless Communications, vol. 14, no. 10, pp. 5350-5359, Oct. 2015, doi: 10.1109/TWC.2015.2436925.

[26] Y. Liu, F. Ji, H. Yu, F. Chen, D. Wan and B. Zheng, "Enhanced Coordinate Interleaved OFDM With Index Modulation," in IEEE Access, vol. 5, pp. 27504-27513, 2017, doi: 10.1109/ACCESS.2017.2777805.

[27] A. T. Dogukan and E. Basar, "Super-Mode OFDM With Index Modulation," in IEEE Transactions on Wireless Communications, vol. 19, no. 11, pp. 7353-7362, Nov. 2020, doi: 10.1109/TWC.2020.3010839.

[28] M. Wen, B. Ye, E. Basar, Q. Li and F. Ji, "Enhanced Orthogonal Frequency Division Multiplexing With Index Modulation," in IEEE Transactions on Wireless Communications, vol. 16, no. 7, pp. 4786-4801, July 2017, doi: 10.1109/TWC.2017.2702618.

[29] J. Choi and Y. Ko, "TCM for OFDM-IM," in IEEE Wireless Communications Letters, vol. 7, no. 1, pp. 50-53, Feb. 2018, doi: 10.1109/LWC.2017.2752168.

[30] A. I. Siddiq, "Low Complexity OFDM-IM Detector by Encoding All Possible Subcarrier Activation Patterns," in IEEE Communications Letters, vol. 20, no. 3, pp. 446-449, March 2016, doi: 10.1109/LCOMM.2015.2514278.

[31] Y. Liu, F. Ji, M. Wen, D. Wan and B. Zheng, "Vector OFDM With Index Modulation," in IEEE Access, vol. 5, pp. 20135-20144, 2017, doi: 10.1109/ACCESS.2017.2756080.

[32] S. Queiroz, J. P. Vilela and E. Monteiro, "Optimal Mapper for OFDM With Index Modulation: A Spectro-Computational Analysis," in IEEE Access, vol. 8, pp. 68365-68378, 2020, doi: 10.1109/ACCESS.2020.2986131.

[33] A. M. Jaradat, J. M. Hamamreh and H. Arslan, "OFDM With Subcarrier Number Modulation," in IEEE Wireless Communications Letters, vol. 7, no. 6, pp. 914-917, Dec. 2018, doi: 10.1109/LWC.2018.2839624.

[34] T. Mao, Q. Wang, J. Quan and Z. Wang, "Zero-Padded Tri-Mode Index Modulation Aided OFDM," GLOBECOM 2017 - 2017 IEEE Global

Communications Conference, Singapore, 2017, pp. 1-5, doi: 10.1109/GLOCOM.2017.8254931.
[35] T. Mao, Q. Wang and Z. Wang, "Generalized Dual-Mode Index Modulation Aided OFDM," in IEEE Communications Letters, vol. 21, no. 4, pp. 761-764, April 2017, doi: 10.1109/LCOMM.2016.2635634.
[36] Y. Shi, X. Lu, K. Gao, J. Zhu and S. Wang, "Subblocks Set Design Aided Orthogonal Frequency Division Multiplexing With All Index Modulation," in IEEE Access, vol. 7, pp. 52659-52668, 2019, doi: 10.1109/ACCESS.2019.2909911
[37] T. Mao, Q. Wang, Z. Wang and S. Chen, "Novel Index Modulation Techniques: A Survey," in IEEE Communications Surveys & Tutorials, vol. 21, no. 1, pp. 315-348, Firstquarter 2019, doi: 10.1109/COMST.2018.2858567.
[38] Z. Yang, F. Chen, B. Zheng, M. Wen and W. Yu, "Carrier Frequency Offset Estimation for OFDM With Generalized Index Modulation Systems Using Inactive Data Tones," in IEEE Communications Letters, vol. 22, no. 11, pp. 2302-2305, Nov. 2018, doi: 10.1109/LCOMM.2018.2869772.
[39] Q. Ma, P. Yang, Y. Xiao, H. Bai and S. Li, "Error Probability Analysis of OFDM-IM With Carrier Frequency Offset," in IEEE Communications Letters, vol. 20, no. 12, pp. 2434-2437, Dec. 2016, doi: 10.1109/LCOMM.2016.2600646.
[40] A. Tusha, S. Doğan and H. Arslan, "Performance Analysis of Frequency Domain IM Schemes under CFO and IQ Imbalance," 2019 IEEE 30th Annual International Symposium on Personal, Indoor and Mobile Radio Communications (PIMRC), Istanbul, Turkey, 2019, pp. 1-5, doi: 10.1109/PIMRC.2019.8904248.
[41] S. Dang, G. Ma, B. Shihada and M. Alouini, "A Novel Error Performance Analysis Methodology for OFDM-IM," in IEEE Wireless Communications Letters, vol. 8, no. 3, pp. 897-900, June 2019, doi: 10.1109/LWC.2019.2899091.
[42] M. Wen, X. Cheng, M. Ma, B. Jiao and H. V. Poor, "On the Achievable Rate of OFDM With Index Modulation," in IEEE Transactions on Signal Processing, vol. 64, no. 8, pp. 1919-1932, April15, 2016, doi: 10.1109/TSP.2015.2500880.
[43] M. Wen, E. Basar, Q. Li, B. Zheng and M. Zhang, "Multiple-Mode Orthogonal Frequency Division Multiplexing With Index Modulation," in *IEEE Transactions on Communications*, vol. 65, no. 9, pp. 3892-3906, Sept. 2017, doi: 10.1109/TCOMM.2017.2710312.
[44] J. Seo, J. Joo, G. Zhu and S. C. Kim, "ESIM OFDM with Schmidl and Cox Algorithm Synchronizer in Rayleigh fading channel," 2019 25th Asia-Pacific Conference on Communications (APCC), Ho Chi Minh City, Vietnam, 2019, pp. 267-270, doi: 10.1109/APCC47188.2019.9026397.
[45] Y. Shi, X. Lu, K. Gao, J. Zhu and S. Wang, "Subblocks Set Design Aided Orthogonal Frequency Division Multiplexing With All Index Modulation," in IEEE Access, vol. 7, pp. 52659-52668, 2019, doi: 10.1109/ACCESS.2019.2909911.
[46] J. Mrkic and E. Kocan, "Hybrid OFDM-IM System for BER Performance Improvement," 2018 26th Telecommunications Forum (TELFOR), Belgrade, 2018, pp. 1-4, doi: 10.1109/TELFOR.2018.8611873.
[47] F. Gao, Y. Zeng, A. Nallanathan, and T.-S. Ng, “Robust Subspace Blind Channel Estimation for Cyclic Prefixed MIMO OFDM Systems: Algorithm, Identifiability and Performance Analysis,” IEEE Journal on Selected Areas in Commun., vol. 26, no. 2, pp. 378-388, Feb. 2008.

Lalitha H is currently pursuing her PhD degree at School of Engineering, Amrita Vishwa Vidyapeetham, Bengaluru. and completed her masters in Digital Electronics and Communication from Visvesvaraya Technological University, India in 2013, obtained her B.E in Instrumentation and Electronics from Bangalore Institute of Technology and her current research includes Signal Processing and frontend design algorithm for WLAN.

Navin Kumar serves as professor at the Department of Electronics and Communication, School of Engineering, Amrita Vishwa Vidyapeetham, Bengaluru. He obtained his Ph. D. in Telecommunication Engineering from the University of Porto, Aveiro and Minho – Portugal, Europe (2007-2011) and M.Tech. in Digital System Engineering from Motilal National Institute of Technology, Allahabad, India in the year 2000. He got his bachelor’s degree in Engineering from the Institution of Electronics and Telecommunication Engineers, New Delhi in 1996. He has over 30 years of working experience in Government, Industry and academia in the IT and Telecommunication area. He has over 10 years of overseas experience in teaching, research and development. He has over 100 publications in peer-reviewed international journals and IEEE conference proceedings. In addition, he has also authored a book and book chapters. His research area includes 5G (mmWave, Architecture and Massive MIMO), Intelligent Transportation Systems, Visible Light Communication, Optical Wireless Communication, IoT & Smart City and Wireless/Mobile Communication and Networking.